

A Remarkably Efficient Azobenzene Peptide for Holographic Information Storage

Palle H. Rasmussen, P. S. Ramanujam, Søren Hvilsted, and Rolf H. Berg*

Contribution from the Risø National Laboratory, DK-4000 Roskilde, Denmark

Received April 24, 1998

Abstract: A new family of proline-based azobenzene peptides (DNO) for holographic information storage is reported. By use of polarization holography, it was found that gratings with extraordinarily high diffraction efficiency (up to 80%) can be recorded in hundreds of milliseconds in a $\sim 13\text{-}\mu\text{m}$ -thick film of dimer **10**. This represents a decrease of the response time by more than 2 orders of magnitude when compared to that of the ornithine-based DNO dimer previously reported. Furthermore, it supports the expectation that increasing the rigidity of the peptide backbone is crucial in the design of effective azobenzene peptides for optical recording. Gratings recorded in **10** can be erased by circularly polarized light in a few seconds. It is also noted that, unlike DNOs previously reported, **10** is soluble in common organic solvents and can be assembled by solution-phase synthesis, which is mandatory for large-scale fabrication.

Introduction

Optical holography^{1,2} provides unique opportunities for storing information at high density and opens up new applications that cannot be contemplated with other techniques. While much attention will continue to be focused on the use of inorganic crystals as erasable holographic storage media, organic materials potentially offer major advantages, such as easy processing and versatility in tailoring of properties. Desirable organic materials should exhibit high diffraction efficiency and fast response, high resolution and permanent storage until erasure, easy erasure, and no high electric field to promote recording or reading, and they should be amenable to large-scale production. Azobenzene polymers,^{3–10} photorefractive polymers,^{11–13} photopolymerizable liquid-crystalline monomers,^{14,15} liquid crystals,¹⁶ and glasses¹⁷ have been investigated

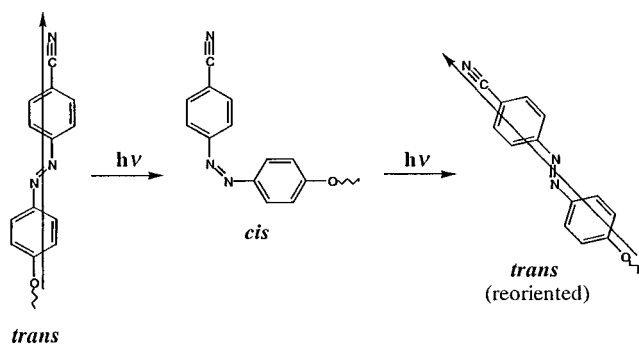


Figure 1. Under illumination ($h\nu = 488\text{ nm}$), the azobenzene chromophore is reversibly isomerized through *trans*–*cis*–*trans* cycles. As a consequence, the chromophore undergoes a number of random reorientations. The optical transition moment axis (the arrow) lies approximately parallel to the long axis of the *trans*-azobenzene.

to fulfill these criteria. The basis for the storage process is a light-induced change in the material's refractive index. In azobenzene polymers, this change can be provided through alignment of the chromophores. Thus, the azobenzene chromophore reorients randomly through a number of laser-induced *trans*–*cis*–*trans* photoisomerization cycles (see Figure 1) until eventually its optical transition moment axis, which lies approximately parallel to the long axis of the *trans*-azobenzene, lies in a plane perpendicular to the polarization direction of the laser beam (see Figure 2). Oriented in this manner, the azobenzene cannot absorb the light and isomerize, and, thus, it will be in a stationary orientation.

Recently, a novel class of oligopeptides with azobenzene chromophores attached to an ornithine-based backbone (DNO, Figure 3) was investigated as new material for holographic information storage.¹⁸ The photochromic properties of azoben-

* Corresponding author. E-mail: rolf.berg@risoe.dk.

- (1) Gabor, D. *Nature* **1948**, *161*, 777–778.
- (2) Gabor, D. *Science* **1972**, *177*, 299–313.
- (3) Eich, M.; Wendorff, J. H.; Reck, B.; Ringsdorf, H. *Makromol. Chem. Rapid Commun.* **1987**, *8*, 59–63.
- (4) Eich, M.; Wendorff, J. H. *Makromol. Chem. Rapid Commun.* **1987**, *8*, 467–471.
- (5) Wiesner, U.; Antonietti, M.; Boeffel, C.; Spiess, H. W. *Makromol. Chem.* **1990**, *191*, 2133–2149.
- (6) Wiesner, U.; Reynolds, N.; Boeffel, C.; Spiess, H. W.; Stumpe, J.; Müller, L.; Kreysig, D.; Hauck, G.; Koswig, H. D.; Ruhmann, R.; Rübner, J. *Makromol. Chem. Rapid Commun.* **1991**, *12*, 81–87.
- (7) Natansohn, A.; Rochon, P.; Gosselin, J.; Xie, S. *Macromolecules* **1992**, *25*, 2268–2273.
- (8) Xie, S.; Natansohn, A.; Rochon, P. *Chem. Mater.* **1993**, *5*, 403–411.
- (9) Hvilsted, S.; Andruzzi, F.; Ramanujam, P. S. *Opt. Lett.* **1992**, *17*, 1234–1236.
- (10) Hvilsted, S.; Andruzzi, F.; Kulinna, C.; Siesler, H. W.; Ramanujam, P. S. *Macromolecules* **1995**, *28*, 2172–2183.
- (11) Ducharme, S.; Scott, J. C.; Twieg, R. J.; Moerner, W. E. *Phys. Rev. Lett.* **1991**, *66*, 1846–1849.
- (12) Liphardt, M.; Goonesekera, A.; Jones, B. E.; Ducharme, S.; Takacs, J.; Zhang, L. *Science* **1994**, *263*, 367–369.
- (13) Meerholz, K.; Volodin, B. L.; Sandalphon; Kippelen, B.; Peyghambarian, N. *Nature* **1994**, *371*, 497–500.
- (14) Zhang, J.; Sponsler, M. B. *J. Am. Chem. Soc.* **1992**, *114*, 1506–1507.
- (15) Zhang, J.; Carlen, C. R.; Palmer, S.; Sponsler, M. *J. Am. Chem. Soc.* **1994**, *116*, 7055–7063.

(16) Wiederrecht, G. P.; Yoon, B. A.; Wasielewski, M. R. *Science* **1995**, *270*, 1794–1797.

(17) Lundquist, P. M.; Wortmann, R.; Geletneky, C.; Twieg, R. J.; Juricj, M.; Lee, V. Y.; Moylan, C. R.; Burland, D. M. *Science* **1996**, *274*, 1182–1185.

(18) Berg, R. H.; Hvilsted, S.; Ramanujam, P. S. *Nature* **1996**, *383*, 505–508.

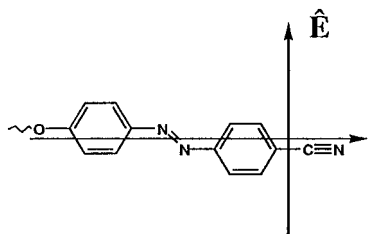


Figure 2. A stationary orientation is obtained when the optical transition moment is oriented in a plane perpendicular to the polarization direction (\hat{E}) of the laser beam.

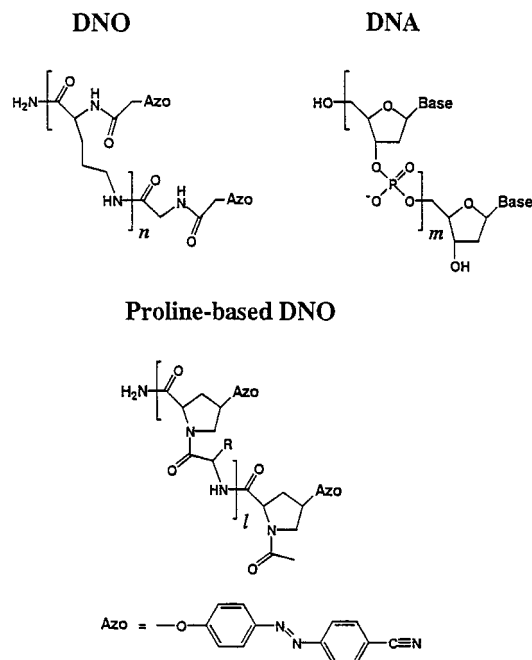


Figure 3. Chemical structures of ornithine-based DNO, DNA, and proline-based DNO.

zene-containing polypeptides, introduced by Goodman and Kossoy more than three decades ago,¹⁹ have been investigated in numerous studies,²⁰ and, in regard to holographic storage, spiropyran-containing polypeptides have been investigated as well.²¹

In analogy to the design of peptide nucleic acids (PNA),^{22–24} DNO²⁵ has a molecular geometry similar to that of DNA. The basic idea underlying the design of DNO was to construct a molecule in which neighboring azobenzene groups are positioned in such a way that the transition moment axes are *nonparallelly* oriented in planes parallel to one another (see Figure 4). This was expected to lead to a more uniform alignment of the chromophores and the backbone since there should be fewer stationary orientations possible. The results showed that holographic gratings with extraordinarily high

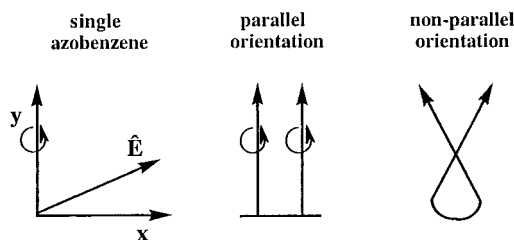


Figure 4. Conceptual model that illustrates the (speculative) rationale behind the DNO design. Assuming that \hat{E} is oriented perpendicular to the plane of the paper, it is then clear that any axis (arrow) lying in the plane of the paper, or in a plane parallel to the paper, will be in a stationary orientation. Thus, in the three cases shown, i.e., the single azobenzene with its optical transition moment lying along the y -axis, the two neighboring azobenzenes held together in a parallel orientation, and the two neighboring azobenzenes stacked on top of each other in a nonparallel orientation, the molecule in question is in a stationary orientation. In all three cases, the molecules can be rotated in the plane of the paper while retaining themselves in a stationary orientation. Furthermore, the single azobenzene can be rotated in any position around its axis while retaining itself in a stationary orientation. Likewise, the two azobenzenes held together in a parallel orientation can be rotated around either one of the axes while retaining the molecule in a stationary orientation. However, if the molecule with the two azobenzenes oriented in a nonparallel manner (i.e., the DNO molecule) is rotated in any position, other than 180° , around either one of its axes, it leads to a situation where the neighboring axis will no longer be oriented in a stationary orientation because it would still be able to undergo photoisomerization cycles. As a result, there should be considerably fewer (“one dimension” less) stationary orientations possible in this case. In other words, with the DNO molecule, a more uniform alignment of the molecule might be expected than in cases where the azobenzenes either are not stacked or are stacked parallel to one another.

diffraction efficiency, which indicates how much of the light entering the sample is diffracted by the holographic gratings, can be recorded in films only a few micrometers thick of a simple dimer ($n = 1$, Figure 3) or longer oligomers. No electric field is required to obtain the high diffraction efficiency, and the holograms, which have lifetimes on the order of years at room temperature, can be erased by exposure to circularly polarized light. In the case of the dimer, it takes about 5 min to obtain a diffraction efficiency of 75%. From both scientific and practical viewpoints, shortening the response time would be highly desirable. In the present study, we sought to modify the backbone in a manner that would permit faster recording.

Experimental Section

General Methods. ^1H NMR and ^{13}C NMR spectra were recorded on a Bruker DPX-250 spectrometer at 300 K. Chemical shifts are expressed as δ values in parts per million (ppm) relative to an internal standard of TMS. NMR spectra were recorded in CDCl_3 unless otherwise indicated. Melting points and glass transitions were determined by differential scanning calorimetry (DSC) of the second heating trace at a rate of $10^\circ\text{C}/\text{min}$.

Materials. All reagents were obtained at highest commercial quality and used without further purification, unless otherwise stated. All solvents used were of superpurity grade.

***N*-Ac-L-*cis*-Hyp-OMe (2).** To a stirred solution of $\text{HCl}\cdot\text{H-L-cis-Hyp-OMe}$ (**1**, 4.0 g, 22.0 mmol) in dioxane– H_2O (1:1, 20 mL) at 0°C was added NaHCO_3 (4.0 g, 47.6 mmol) in small portions over 10 min, together with acetic anhydride (2.32 mL, 24.5 mmol) in dioxane– H_2O (1:1, 5.0 mL), dropwise over 30 min. After 2 h at 25°C , the resulting solution was concentrated in vacuo, diluted with saturated aqueous NaCl (20 mL), and extracted with CHCl_3 (10×15 mL). The pooled extracts were dried (MgSO_4) and concentrated to a clear oil. Yield: 4.0 g (97%). ^1H NMR: δ 1.95 (s, 1H), 2.05 (s, 3H), 2.30 (m, 2H), 3.60 (m, 2H), 3.71 (s, 3H), 4.36 (m, 1H), 4.42 (m, 1H). ^{13}C NMR: δ 21.95, 37.06, 52.47, 56.16, 57.22, 70.50, 169.87, 173.88.

(19) Goodman, M.; Kossoy, A. *J. Am. Chem. Soc.* **1966**, *88*, 5010–5015.

(20) For a recent review, see: Pieroni, O.; Fissi, A.; Popova, G. *Prog. Polym. Sci.* **1998**, *23*, 81–123.

(21) Cooper, T. M.; Tondigli, V.; Natarajan, L. V.; Shapiro, M.; Obermeier, K.; Crane, R. L. *Appl. Opt.* **1993**, *32*, 674–677.

(22) Nielsen, P. E.; Egholm, M.; Berg, R. H.; Buchardt, O. *Science* **1991**, *254*, 1497–1500.

(23) Egholm, M.; Buchardt, O.; Nielsen, P. E.; Berg, R. H. *J. Am. Chem. Soc.* **1992**, *114*, 1895–1897.

(24) Egholm, M.; Nielsen, P. E.; Buchardt, O.; Berg, R. H. *J. Am. Chem. Soc.* **1992**, *114*, 9677–9678.

(25) We have chosen to call this type of structures DNO since the azobenzene peptides used in the previous work (ref 18) were all based on diamino acid N^α -substituted oligopeptides.

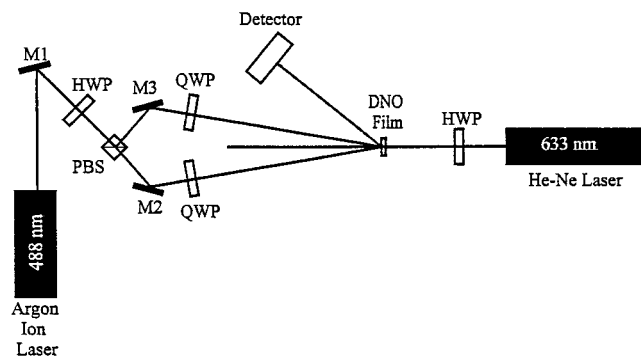
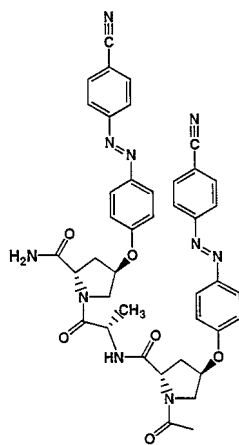


Figure 5. Experimental setup for polarization holography. M1, M2, and M3 are mirrors; HWP, half-wave plate; QWP, quarter-wave plates; PBS, polarization beam-splitter; D, detector.

Chart 1



10

4-[(E)-2-(4-Hydroxyphenyl)-1-diazenyl]benzonitrile (3). To a solution of 4-aminobenzonitrile (7.08 g, 0.06 mol) in 99% ethanol (60 mL) was added 6 N HCl (100 mL), causing immediately a precipitate. The ethanol was removed in vacuo at maximum 55 °C. After the mixture was stirred for 10 min at 0 °C, a precooled (0 °C) solution of NaNO₂ (4.14 g, 0.06 mol) in H₂O (60 mL) was added dropwise, constantly keeping the temperature below 5 °C. The cold mixture was added dropwise to a solution of phenol (5.64 g, 0.06 mol) in 3 N NaOH (200 mL), constantly keeping the temperature between -5 and -1 °C. The reaction mixture was stirred for 1 h and left for 16 h. The precipitate was washed with H₂O, dissolved in 50% aqueous ethanol (800 mL), and then precipitated with 12 N HCl, filtrated, and air-dried. Yield: 11.3 g (84%), mp 190 °C. ¹³C NMR (DMSO-*d*₆): δ 112.15, 116.10, 118.42, 122.64, 125.48, 133.41, 145.34, 154.31, 162.08.

N-Ac-L-trans-Pro(4-{4-[(E)-2-(4-cyanophenyl)-1-diazenyl]phenoxy})-O-Me (4). To a stirred solution of compound **2** (3.90 g, 20.8 mmol), compound **3** (7.10 g, 31.7 mmol, 1.5 equiv), and PPh₃ (6.11 g, 23.3 mmol, 1.1 equiv) in dry THF (50 mL) was added at 0 °C diethyl azodicarboxylate (DEAD) (3.66 mL, 23.3 mmol, 1.1 equiv), and the mixture was stirred at 23 °C for 16 h under argon. The resulting suspension was filtered, and the remanance was washed with cold THF (0 °C, 10 mL) and dried. Yield: 6.80 g (83%). ¹H NMR: δ 2.15 (s, 3H), 2.55 (m, 2H), 3.75 (s, 3H), 3.91 (m, 2H), 4.80 (bd, 1H, *J* = 10 Hz), 5.20 (bs, 1H), 6.97 (d, 2H, *J* = 8.9 Hz), 7.82 (d, 2H, *J* = 8.6 Hz), 7.97 (d, 4H, *J* = 8.7 Hz). ¹³C NMR: δ 22.28, 34.89, 52.38, 53.00, 57.05, 76.01, 113.50, 115.81, 118.53, 123.14, 125.51, 133.17, 147.31, 154.61, 159.68, 169.43, 171.19.

N-Ac-L-trans-Pro(4-{4-[(E)-2-(4-cyanophenyl)-1-diazenyl]phenoxy})-OH (5). To a stirred solution/suspension of **4** (6.62 g, 16.9 mmol) in THF (150 mL) at 0 °C was added LiOH (611 mg, 25.5 mmol, 1.5 equiv) in water (50 mL), and the mixture was stirred for 16 h at 5 °C. The mixture was acidified with 10% aqueous citric acid to pH ~3 and extracted with chloroform (4 × 200 mL). The combined organic

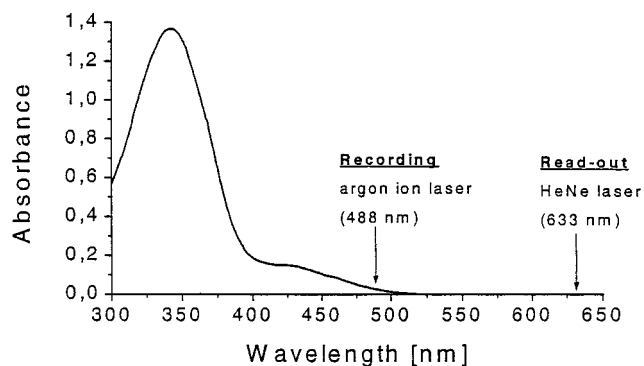


Figure 6. UV-visible absorption spectrum of **10** coated as a very thin film (approximately 100 nm thick) on a glass substrate.

phases were concentrated to an orange solid, which was dissolved in chloroform-methanol (4:1, ~50 mL) and purified on basic alumina with chloroform (350 mL), 10% citric acid (350 mL), and methanol-chloroform (1:4, 250 mL) as eluents. Yield: 6.0 g (94%). ¹H NMR (DMSO-*d*₆): δ 2.01 (s, 3H), 2.30 (m, 1H), 2.60 (m, 1H), 3.80 (d, 1H, *J* = 11.52 Hz), 3.95 (d, 1H, *J* = 4.13 Hz), 4.33 (t, 1H, *J* = 7.96 Hz), 5.28 (bs, 1H), 7.22 (d, 2H, *J* = 8.77 Hz), 7.96 (bd, 4H, *J* ≈ 8.6 Hz), 8.05 (d, 2H, *J* = 8.41 Hz). ¹³C NMR (DMSO-*d*₆): δ 22.09, 34.62, 52.78, 57.12, 76.29, 112.63, 116.15, 118.46, 122.91, 125.30, 133.73, 146.41, 154.10, 160.33, 168.54, 172.91.

N-Boc-L-trans-Pro(4-{4-[(E)-2-(4-cyanophenyl)-1-diazenyl]phenoxy})-O-Me (7). To a stirred solution of methyl *N*-Boc-*cis*-4-hydroxy-L-prolinate **6** (5.0 g, 20.38 mmol), compound **3** (5.92 g, 26.50 mmol, 1.5 equiv), and PPh₃ (5.88 g, 22.40 mmol, 1.1 equiv) in dry THF (100 mL) was added at 0 °C diethyl azodicarboxylate (DEAD) (3.53 mL, 22.40 mmol, 1.1 equiv), and the mixture was stirred at 23 °C for 16 h under argon. The mixture was concentrated in vacuo to a red oil, which was dissolved in chloroform (~15 mL) and run through basic alumina using chloroform as eluent. The resulting solution was concentrated in vacuo to an orange solid, which was purified by flash chromatography on a silica column (3 × 18 cm) using methylene chloride-diethyl ether (9:1) as eluent. Yield: 7.5 g (82%). ¹H NMR: δ 1.40 (s, 9H), 2.55 (m, 2H), 3.75 (s, 3H), 3.85 (m, 2H), 4.55 (m, 1H), 5.02 (m, 1H), 6.94 (d, 2H, *J* = 8.6 Hz), 7.80 (d, 2H, *J* = 8.5 Hz), 7.95 (bd, 4H, *J* = 8.5 Hz). ¹³C NMR: δ 28.02, 35.20, 51.94, 52.90, 57.58, 74.72, 80.12, 112.91, 115.53, 119.73, 122.76, 125.13, 132.92, 146.67, 154.14, 159.96, 170.64, 172.57.

N-Boc-L-Ala-L-trans-Pro(4-{4-[(E)-2-(4-cyanophenyl)-1-diazenyl]phenoxy})-O-Me (8). Compound **7** (4.0 g, 8.88 mmol) was stirred in trifluoroacetic acid-methylene chloride (1:1, 100 mL) at 0 °C for 1.5 h. The mixture was concentrated in vacuo and coevaporated with benzene-methylene chloride (1:1, 3 × 50 mL) to a red oil, which was dissolved in dry THF (100 mL). Boc-L-Ala-OH (1.68 g, 8.88 mmol), 1-hydroxybenzotriazole (HOBt) (1.20 g, 8.88 mmol), and Et₃N (5.1 mL, 26.6 mmol, 3.3 equiv) were added, and the mixture was cooled to 0 °C. 1-Ethyl-3-(3'-dimethylaminopropyl)carbodiimide hydrochloride (WSC·HCl) (2.16 g, 11.28 mmol, 1.27 equiv) was added, and the mixture was stirred for 16 h at 20 °C under argon. The mixture was concentrated in vacuo to a red oil, which was dissolved in chloroform (100 mL) and washed with water (3 × 100 mL). The organic phase was concentrated to a foam, which was purified by flash chromatography on a silica column (5 × 18 cm) using chloroform-methanol (95:5) to a red solid. Yield: 4.45 g (96%). ¹H NMR: δ 1.37 (d, 3H, *J* = 7.1 Hz), 1.40 (s, 9H), 2.28 (m, 1H), 2.63 (m, 1H), 3.78 (s, 3H), 3.95 (dd, 1H, *J* = 4.3 + 11.3 Hz), 4.06 (d, 1H, *J* = 11.3 Hz), 4.47 (p, 1H, *J* = 7.5 Hz), 4.71 (t, 1H, *J* = 8.2 Hz), 5.14 (bs, 1H), 5.39 (d, 1H, *J* = 7.8 Hz), 6.97 (d, 2H, *J* = 8.9 Hz), 7.79 (d, 2H, *J* = 8.5 Hz), 7.95 (dd, 4H, *J* = 8.5 + 8.9 Hz). ¹³C NMR: δ 18.33, 28.28, 34.55, 47.79, 52.24, 52.50, 57.73, 75.90, 79.65, 113.40, 115.69, 118.56, 123.14, 125.56, 133.16, 147.31, 154.58, 155.01, 159.77, 171.84, 172.05.

N-Boc-L-Ala-L-trans-Pro(4-{4-[(E)-2-(4-cyanophenyl)-1-diazenyl]phenoxy})-NH₂ (9). Compound **8** (4.0 g, 7.67 mmol) was dissolved in a solution of ammonia in methanol (8 M, 200 mL) and stirred for 12 h at 60 °C. The mixture was concentrated in vacuo to a red solid.

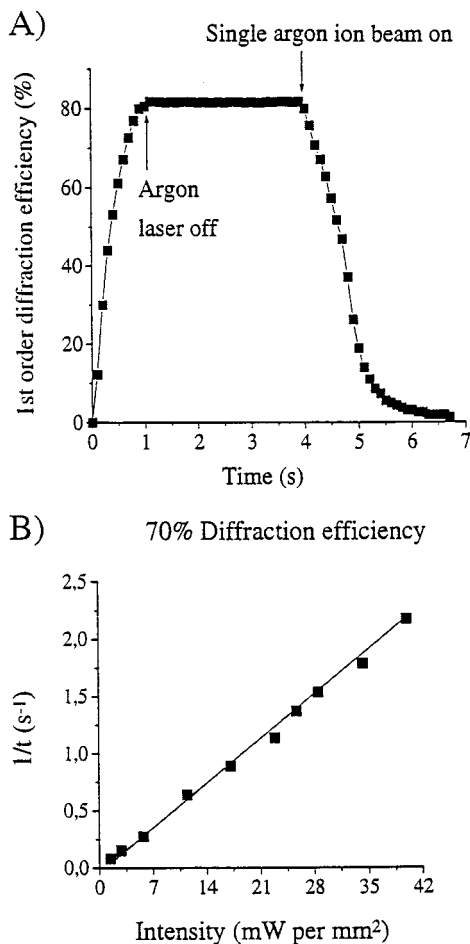


Figure 7. (A) First-order diffraction efficiency as a function of time, measured during the grating formation in $\sim 13\text{-}\mu\text{m}$ -thick film of **10**. From the observed diffraction efficiency of 80% and a film thickness of about $10\ \mu\text{m}$, an index modulation of approximately 0.08 at 633 nm can be calculated, assuming that diffraction is due to change in refractive index alone. (B) Plot of $1/t$ (reciprocal time to reach 70% diffraction efficiency) against intensity for **10**.

Yield: 3.88 g (>99%). ^1H NMR: δ 1.35 (d, 3H, $J = 6.8$ Hz), 1.40 (s, 9H), 2.38 (m, 1H), 2.68 (m, 1H), 3.95 (m, 2H), 4.49 (t, 1H, $J = 6.8$ Hz), 4.79 (dd, 1H, $J = 6.3 + 7.8$ Hz), 5.21 (m, 1H), 5.51 (d, 1H, $J = 7.8$ Hz), 6.13 (m, 1H), 7.01 (d, 2H, $J = 8.9$ Hz), 7.77 (d, 2H, $J = 8.5$ Hz), 7.93 (dd, 4H, $J = 8.5 + 8.9$ Hz). ^{13}C NMR: δ 18.10, 28.23, 33.39, 47.92, 52.16, 58.35, 75.92, 79.73, 113.26, 115.66, 118.47, 123.04, 125.45, 133.06, 147.13, 154.51, 155.01, 160.05, 172.78, 172.94.

N-Ac-*L*-*trans*-Pro(4-{4-[(*E*)-2-(4-cyanophenyl)-1-diazenyl]phenoxy})-*L*-Ala-*L*-*trans*-Pro(4-{4-[(*E*)-2-(4-cyanophenyl)-1-diazenyl]phenoxy})-NH₂ (**10**). Compound **9** (2.0 g, 3.95 mmol) was stirred in trifluoroacetic acid–methylene chloride (1:1, 100 mL) at 0 °C for 1.5 h. The mixture was concentrated in vacuo and coevaporated with benzene–methylene chloride (1:1, 3 \times 50 mL). The resulting red oil was dissolved in methylene chloride (200 mL), and Et₃N (2.0 mL, 11.8 mmol, 3.0 equiv) was added. A solution of **5** (1.79 g, 4.74 mmol, 1.2 equiv), Et₃N (2.0 mL, 11.8 mmol, 3.0 equiv), and benzotriazol-1-yloxytris(dimethylamino)phosphonium hexafluorophosphate (BOP) (2.09 g, 4.74 mmol, 1.2 equiv) in methylene chloride (200 mL) was added, and the mixture was stirred for 12 h. The mixture was concentrated in vacuo to approximately 15 mL and purified by flash chromatography on a basic alumina column (4 \times 3 cm) using chloroform–methanol (85:15) as eluent. The resulting mixture was concentrated in vacuo to a red solid, which was dissolved in ethyl acetate (150 mL) and washed with aqueous KHSO₄ (10% w/w, 2 \times 100 mL), water (2 \times 100 mL), and aqueous NaHCO₃ (2 \times 100 mL), dried with MgSO₄, and concentrated to a red solid. Yield: 2.65 g (88%). ^1H NMR (CDCl₃): δ 1.40 (d, 3H, $J = 6.4$ Hz), 2.06 (s, 3H), 2.4–2.7 (m, 4H), 3.87–4.05

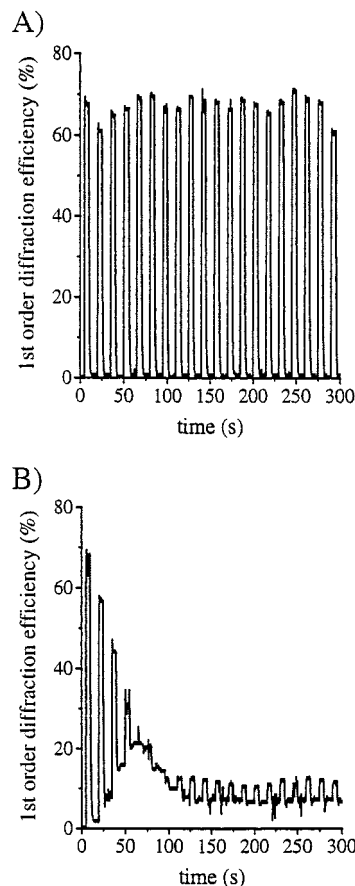


Figure 8. Recording–erasure cycles in a $\sim 13\text{-}\mu\text{m}$ -thick film of **10** irradiated from (A) the glass side and (B) the film side.

(m, 4H), 4.70 (m, 3H), 5.05 (m, 1H), 5.18 (m, 1H), 6.97 (m, 4H), 7.75 (m, 4H), 7.90 (m, 8H). ^{13}C NMR (CDCl₃): δ 17.24, 22.22, 33.80, 33.81, 47.15, 52.33, 53.06, 58.48, 59.27, 75.63, 75.91, 113.22, 115.48, 115.58, 118.44, 123.01, 125.41, 133.04, 146.99, 154.36, 159.75, 159.98, 170.26, 170.60, 171.91, 173.07. MALDI-TOF-MS (DHB): m/z ($M + H^+$) found (calcd) 768.2 (767.8).

Preparation of DNO Films. Films were prepared by dissolving 25 mg of DNO in a solution of hexafluoro-2-propanol–trifluoroacetic acid–methylene chloride (76:18:6 (v/v/v), 400 μL). The resulting red solution was filtered through a syringe filter (0.7 μm pore size). Next, 10–14 drops of the solution were cast on a glass plate (20 mm in diameter) in a desiccator, and vacuum was immediately applied. The film was dried for 30 min in the desiccator and then transferred to an oven at 90 °C overnight. The thickness of the film in question was measured with a Dektak profiler. Films with a thickness ranging from 1 to 15 μm were prepared to produce the reference curve shown in Figure 7. The thickness of the individual films examined typically had a variation in the thickness of less than $\pm 3\%$.

Results and Discussion

It was envisioned from previous work¹⁸ that constraining the conformational freedom of the DNO backbone structure would lead to a more efficient alignment of the neighboring chromophores. It appears logical that the *coordinated* reorientation of chromophores in a molecule will be more efficient the more strongly or more rigidly the chromophores are held together. Based on this rationale, proline-based DNO, shown schematically in Figure 3, was designed. While retaining a similar molecular geometry, the proline-based backbone would be more rigid than the ornithine-based one due to the pyrrolidine ring, which also mimics the sugar ring of the DNA

(26) Merrifield, R. B. *J. Am. Chem. Soc.* **1963**, *85*, 2149–2154.

(27) Merrifield, B. *Science* **1986**, *232*, 341–347.

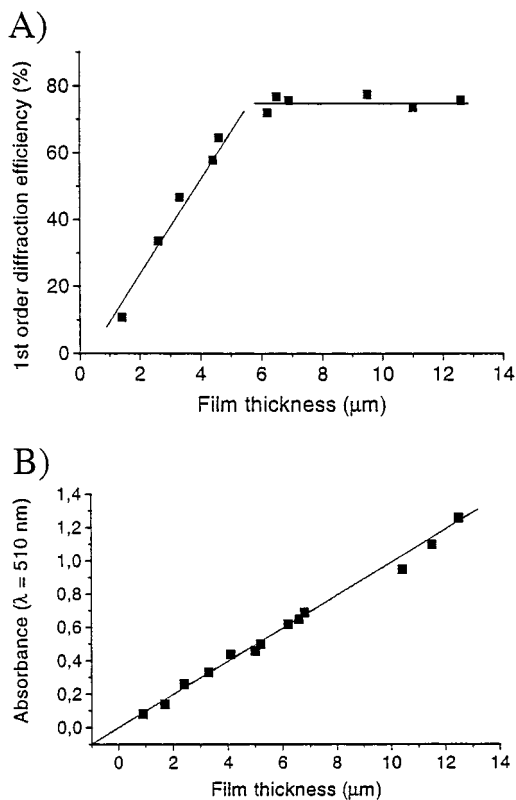


Figure 9. (A) Maximum first-order diffraction efficiency obtained (after ~1 s) as a function of film thickness. (B) Absorbance at 510 nm as a function of film thickness.

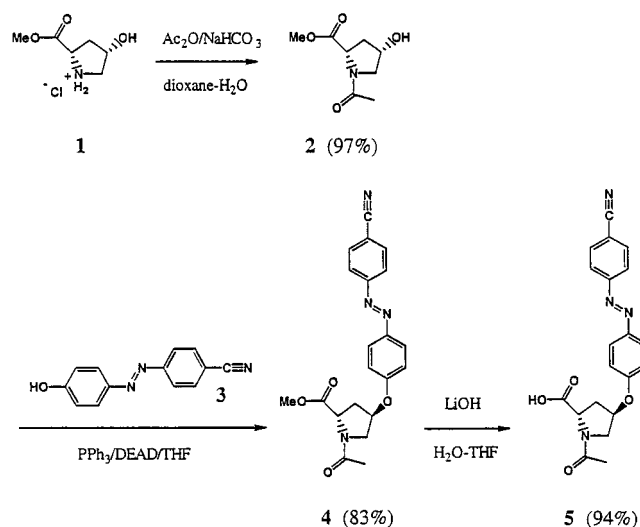
backbone structure. A series of proline-based DNOs was prepared by Merrifield solid-phase synthesis,^{26,27} and their recording properties were examined by polarization holography.²⁸ Films of good optical quality with a thickness of approximately 10 μm were obtained from hexafluoro-2-propanolic solutions. When the films were examined in a polarization microscope, they exhibited no birefringence. The setup used for conventional two-beam polarization holography is shown in Figure 5.²⁹ Two orthogonally circularly polarized beams at 488 nm from an argon ion laser, with a total intensity of 25 mW/mm², were used to record holographic gratings in the film. The spacing of the gratings is about 3.7 μm, and the spot size is about 3 mm in diameter. A circularly polarized beam at 633 nm from a 4.2-mW helium–neon laser was used for read-out. DNOs were tested, with the best one identified from this series as dimer **10** (Chart 1).³⁰ The UV–visible absorption spectrum of dimer **10** is shown in Figure 6, and as shown in Figure 7A, it gave a first-order diffraction efficiency of 75% in about 800 ms. The maximum efficiency, approximately 80%, was reached in about 1 s. At recording times longer than 1 s, the efficiency is lowered. The response of **10** is more than 350 times faster than that of the ornithine-based dimer. After exposure, the illuminated film, when examined between crossed polarizers, exhibits birefringence. The diffraction efficiency remained stable

(28) It is not necessary to use polarization holography for these materials. It is possible to record with the same polarization. However, the diffraction efficiency varies according to the polarization combination. It is possible to achieve 100% diffraction efficiency with two orthogonally circularly polarized beams for the writing and one circularly polarized beam for the read out, even in thin films. See, e.g.: Todorov, T.; Nikolova, L.; Tomova, N. *Appl. Opt.* **1984**, *23*, 1342.

(29) A general discussion on interference, diffraction, and holography can be found in the following: Collier, R. J.; Buckhardt, C. B.; Lin, L. H. *Optical Holography*; Academic Press: New York, 1971.

(30) The synthesis and recording properties of the complete series will be reported elsewhere.

Scheme 1

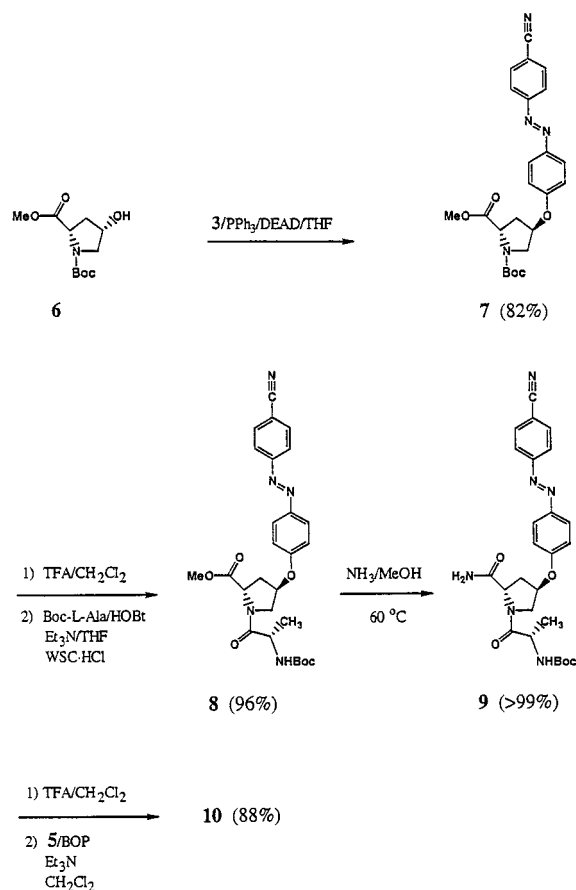


after the two beams from the argon ion laser were switched off, and, after 3 s, one of the argon ion beams (12.5 mW/mm²) was switched on again. The diffraction efficiency decreased rapidly and reached a level of 1.2% in less than 3 s. It is noted that the erasure process is much faster than that previously observed with ornithine-based DNO. The duration of the exposure required to reach a certain diffraction efficiency is inversely proportional to the intensity of the recording beams over a wide range, indicating that no significant thermal effects are involved in the recording process. Thus, a plot of the reciprocal of the time it takes to reach 70% diffraction efficiency against the intensity of the laser power gave a straight line (Figure 7B). For holograms recorded in **10**, with an exposure time of about 1 s, lifetimes of now more than 1 year have been observed. The holograms can be erased thermally if heated to about 110 °C. No first-order thermal transitions were detected, by differential scanning calorimetry, in the temperature range from 25 °C to the decomposition temperature (about 220 °C). However, a glass transition was observed at around 116 °C, suggesting that the material is amorphous.

As shown in Figure 8A, recording–erasure cycles can be performed in a film of **10** if the film-coated glass is irradiated through the glass side. If the film was irradiated directly, that is, from the film side, the first-order diffraction efficiency decreased rapidly after a few cycles (see Figure 8B) as the diffraction was spread into other orders. This is due to a large surface relief, which is created when the film is irradiated from the film side, as seen by using atomic force microscopy (not shown). An obvious explanation of the surface relief is to be found in the role played by the free surface. When the laser beams enter from air into the film, the first surface is the free surface of the film. Due to the higher intensity, a surface relief is likely to occur at this surface. On the other hand, when the laser beams enter the film through the glass surface, the first film surface is the surface in contact with the glass. No surface relief is possible at this interface. When the beams leave the free surface of the film, their intensity has decreased due to the absorption in the film. The surface relief has thus an extremely low magnitude. Studies are currently underway to examine this phenomenon. In Figure 9A, it is seen that the first-order diffraction efficiency decreases rapidly if the film thickness becomes less than 5 μm. The reference curve shown in Figure 9B can be used for indirectly estimating the thickness of a film.

Another important factor for the development of holographic recording materials is the ease of their preparation for large-

Scheme 2



scale availability. Because of their insolubility in organic solvents other than trifluoroacetic acid and hexafluoro-2-propanol, the ornithine-based DNOs could only be assembled by solid-phase synthesis, which is difficult to scale-up to multigram or larger quantities. By contrast, the proline-based ones are soluble in methylene chloride, chloroform, acetonitrile, and other solvents compatible with solution-phase synthesis. This unexpected property greatly facilitates large-scale fabrication, which is a prerequisite for the production of low-cost materials. A solution-phase synthetic strategy was developed, and **10** was synthesized on a 3-g scale from commercially available hydroxyproline derivatives through the procedure outlined below. A key step involves stereospecific substitution of the hydroxy group of **2** and **6**, which has the (*S*)-configuration

(31) Mitsunobu, O. *Synthesis* **1981**, 1–28.

(32) Peyghambarian, N.; Kippelen, B. *Nature* **1996**, *383*, 505.

(33) Berg, R. H.; Almdal, K.; Batsberg Pedersen, W.; Holm, A.; Tam, J. P.; Merrifield, R. B. *J. Am. Chem. Soc.* **1989**, *111*, 8024–8026.

(34) Rigby, P. *Nature* **1996**, *384*, 610.

in the pyrrolidine ring, with an azobenzene chromophore in the (*R*)-configuration using the Mitsunobu reaction.³¹ Synthesis of the two building blocks **5** (Scheme 1) and **9** (Scheme 2) was readily accomplished in three and four steps, respectively, and in 76% and 79% overall yields, respectively. After deprotection of the Boc group, **9** was coupled to **5**, providing **10** in 88% yield. The peptide was characterized by ¹H and ¹³C nuclear magnetic resonance spectroscopy and shown to have the expected molecular mass by matrix-assisted laser desorption/ionization time-of-flight mass spectrometry. Small amounts of impurities could be detected by high-performance liquid chromatography (HPLC). A small fraction of **10** was purified by HPLC, but this did not lead to any improvement of the recording properties, indicating that the behavior of **10** is not affected significantly by the presence of impurities. Since **10** contains proline residues, studies are in progress to investigate the possible *cis*–*trans* isomerization of the peptide bonds.

Conclusion

In summary, a strategy that focuses on increasing the rigidity of the backbone has led to the design of a new class of azobenzene peptides that eliminates some of the limitations associated with the first generation of DNOs. With regard to the response time, by adding further structural constraints to the molecule, there may be a good deal of room for further improvement. For potential use in volume holography, recording in thick films of the order of 1 mm is needed.³² The greatly improved solubility properties of **10** should increase the chance of finding a polymer host more suitable for “dilution” of DNO than the previously reported one consisting of polystyrene-grafted polyethylene.^{18,33} Besides peptides, the work described here suggests that a wide range of other small and rationally designed, rigid azobenzene molecules may prove valuable for holographic storage of information. Widespread applications of any azobenzene system will rely on the commercial production of blue laser diodes, which is expected to be realized in the very near future.³⁴

Acknowledgment. This paper is dedicated to Professor James P. Tam on the occasion of his 50th birthday. We thank Dr. Walther Batsberg Pedersen for his expert assistance in chromatography. We thank Ms. Anne Bønke Nielsen and Ms. Britt J. Harder for skilled technical assistance. This work was supported by the Danish Natural Science Research Council and the Danish Materials Technology Development Program, and by a Ph.D. grant from the Danish Research Academy (P.H.R.).

Supporting Information Available: Details of the solution-phase synthesis of dimer **10** (PDF). This material is available free of charge via the Internet at <http://pubs.acs.org>.

JA981402Y